MEASUREMENTS OF VELOCITY-ACCELERATION STATISTICS IN TURBULENT BOUNDARY LAYERS

K. Todd Lowe
Roger L. Simpson

Department of Aerospace and Ocean Engineering,
Virginia Tech
Blacksburg, Virginia 24061, USA

ABSTRACT

An advanced laser Doppler velocimetry system is developed to acquire measurements of fluctuating velocity-acceleration statistics in turbulent boundary layers. The measurements give important insight into the near-wall turbulence structure since the statistical correlations of interest, $\overline{u_i a_j}$ appear directly in the Reynolds stress transport equations as a sum of the velocity-pressure gradient correlation, $\frac{1}{\rho}\left(\overline{u_i \frac{\partial p}{\partial x_j}} + u_j \frac{\partial p}{\partial x_i}\right)$, the dissipation rate, $2\nu\overline{\frac{\partial u_i}{\partial x_k}\frac{\partial u_j}{\partial x_k}}$, and the viscous diffusion, $\nu\nabla^2\overline{u_i u_j}$. The immediate power of such measurements is that combinations of terms in the Reynolds stress transport equation may be characterized by a single statistical measurement at one location in the flow—no gradients need be computed. In the present paper, data are presented for a constant-pressure 2D turbulent boundary layer at $Re_\theta = 6800$. Near-wall results for the dominant term in the velocity-acceleration tensor, the streamwise correlation $\overline{ua_x}$, compare favorably with DNS for the same quantity at $Re_\theta = 1410$ and $Re_\tau = 640$; furthermore, the quantity exhibits no Reynolds number effects within experimental uncertainties. This study exhibits the potential of the technique to be applied to more complex flows, particularly those 3D separating flows in which the motions contributing to the velocity-acceleration correlations become dominant.

INTRODUCTION

Interest in Lagrangian acceleration measurement has been growing with the advent of some new optical particle tracking technologies and the increased computational and storage capacities of modern computers and digital signal processors. Due to the complexity of the measurements, very little information exists about the acceleration structure in turbulent flows. Published techniques include indirect measurement via the isotropy assumption by measuring the fourth-order velocity structure functions (Hill and Thoroddsen, 1997), as well as direct studies using DNS (Vedula and Yeung, 1999), particle tracking velocimetry techniques (Virant and Dracos, 1997; LaPorta et al., 2001; Voth et al., 1998, 2002), particle image velocimetry (PIV) (Christensen and Adrian, 2002), and laser Doppler velocimetry (LDV) (Lehmann et al. 2002). In the current study, LDV is chosen primarily due to its exceptional resolution in the near wall region.

Previous work has shown the potential for estimating instantaneous particle accelerations using LDV. The differential LDV technique can be directly extended to make acceleration measurements by simply adjusting the signal processing. In work reported by Lehmann et al. (2002), the authors compared three methods for estimating particle accelerations and used one of the techniques in a flow situation. The results validated that LDV could successfully be extended to acquire acceleration measurements in turbulent flows.

Of particular interest in the current study is the role of the correlation between the fluctuating velocity and fluctuating acceleration in the Reynolds stresses transport (RST) equations. This term is chosen for two reasons, first because it appears directly in the RST equations as a combination of up-to-now difficult to measure terms. Second because the correlation results in low uncertainties relative to the individual uncertainties of the velocities and the accelerations, since the random noise content will not result in any net correlation.

The relationship between the velocity-acceleration correlation and the Reynolds stress transport may be seen through an analysis of the Navier-Stokes equations. A basic, *linear* form of these equations is

$$\mathrm{A}_i = -\frac{1}{\rho}\frac{\partial \mathrm{P}}{\partial x_i} + \nu\nabla^2 U_i \tag{1}$$

where A_i is the Lagrangian fluid particle acceleration. Since this equation is linear, the fluctuating form is analogous. By multiplying the fluctuating form of equation (1) by the fluctuating velocity u_j and Reynolds averaging one obtains

$$\overline{a_i u_j} = -\frac{1}{\rho}\overline{u_j \frac{\partial p}{\partial x_i}} + \nu\overline{u_j \nabla^2 u_i} \tag{2}$$

By switching the indices in equation (2) and adding the result back with the original equation, the following form results:

$$\overline{a_i u_j} + \overline{a_j u_i} = -\frac{1}{\rho}\overline{u_j \frac{\partial p}{\partial x_i} + u_i \frac{\partial p}{\partial x_j}} + \nu\overline{u_j \nabla^2 u_i + u_i \nabla^2 u_j} \tag{3}$$

The final term on the right hand side of this equation may be decomposed into dissipative and diffusive terms, as shown by Pope (2000):

$$\nu\overline{u_j \nabla^2 u_i + u_i \nabla^2 u_j} = -2\nu\overline{\frac{\partial u_i}{\partial x_k}\frac{\partial u_j}{\partial x_k}} + \nu\nabla^2\overline{u_i u_j} \tag{4}$$

which appear directly in the RST equations given as:

$$\frac{\partial \overline{u_i u_j}}{\partial t} + U_k\frac{\partial \overline{u_i u_j}}{\partial x_k} + \frac{\partial \overline{u_i u_j u_k}}{\partial x_k} = -\overline{u_i u_k}\frac{\partial U_j}{\partial x_k} - \overline{u_j u_k}\frac{\partial U_i}{\partial x_k} - \frac{1}{\rho}\left(\overline{u_i \frac{\partial p}{\partial x_j} + u_j \frac{\partial p}{\partial x_i}}\right) - 2\nu\overline{\frac{\partial u_i}{\partial x_k}\frac{\partial u_j}{\partial x_k}} - \nu\nabla^2\overline{u_i u_j} \tag{5}$$

In this way, the velocity-acceleration tensor is directly related to the RST equations by the sum of the velocity-pressure gradient correlation, $\Pi_{ij} = \frac{1}{\rho}\left(\overline{u_i \frac{\partial p}{\partial x_j} + u_j \frac{\partial p}{\partial x_i}}\right)$, viscous diffusion, $D_{ij} = \nu\nabla^2\overline{u_i u_j}$, and dissipation rate, $\epsilon_{ij} = -2\nu\overline{\frac{\partial u_i}{\partial x_k}\frac{\partial u_j}{\partial x_k}}$ tensors. Thus the velocity-acceleration fluctuation correlation measurements give a second equation (apart from equation (5) itself) for determining Π_{ij} when measurements for D_{ij} and ϵ_{ij} are possible. The importance of the velocity-pressure gradient term in complex flows has been shown for low Reynolds numbers by the DNS of Colman et al. (2000). In the strained channel flow DNS, the authors discovered that Π_{ij} is of primary importance to the evolution of the Reynolds stresses. They showed that the lag between the mean shear rate and the Reynolds shear stresses, a key problem in 3D flows, is primarily due to this term.

In this paper, we wish to utilize the capabilities of a new advanced LDV for velocity-acceleration correlation measurements in a 2D constant pressure turbulent boundary layer at $Re_\theta = 6800$. This simplest of turbulent boundary layer flows has been the subject of many experimental studies in the past. DeGraaff and Eaton (2000) give an extensive review of the work that to this point has primarily involved the measurement of velocity statistics. The velocity-acceleration measurements add to the database of information on this flow and give insight into the mechanisms leading to Reynolds stress transport.

APPARATUS AND INSTRUMENTATION

Measurements were taken in the turbulent boundary layer of the Aerospace and Ocean Engineering Department small boundary layer wind tunnel. A detailed description of this facility in its present configuration is given by Bennington (2004). The nominal dimensions of the test section are $23cm$ wide by $10cm$ high by $2m$ long. The measurements were acquired $1.16m$ downstream of the contraction on the centerline of the tunnel. The floor boundary layer was tripped to turbulence using a pair of square bars with edges of $0.32cm$ spanning the width of tunnel floor. The two bars were spaced by $20cm$ with 20 grit sand paper attached to the floor between the bars. The measurements were acquired at over 350 bar-heights downstream of the trip arrangement, resulting in a fully relaxed boundary layer. The current measurements showed the inviscid core of the wind tunnel to have a velocity of $26.9m/s$ with 0.3% turbulence intesity and another 0.7% low frequency unsteadiness. The unsteadiness was found to be below $10Hz$ and thus did not correlate with the higher-frequency turbulence in the boundary layer.

The measurements were acquired using an advanced 3D laser Doppler velocimetry system. A perspective schematic view of the probe is given in figure 1. The LDV utilizes six laser beams, two each of $476.5nm$, $488nm$ and $514.5nm$ wavelengths. The beams are conditioned on a remote optical table where one beam for each of the three wavelengths are frequency shifted using Bragg cells. The shifts are $40MHz$, $80MHz$, and $60MHz$ for the $476.5nm$, $488nm$ and $514.5nm$ wavelengths, respectively. The conditioned beams are coupled into six polarization preserving fiber optics with $4\mu m$ diameter cores. The six fibers are mounted into three independently-adjustable optics heads beneath the wind tunnel. The light from the fibers are collimated at $1.3mm$ diameter and three

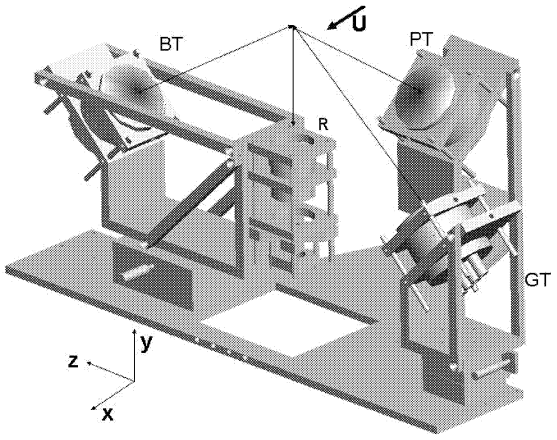

Figure 1: Schematic of the LDV probe; BT: $488nm$ transmitting optics, GT: $514.5nm$ transmitting optics, PT: $476.5nm$ transmitting optics, R: receiving optics. Tunnel coordinates are given.

achromatic lenses are used to focus the pairs of beams to a diffraction-limited spot size of approximately $125\mu m$ in the measurement volume. The pairs of beams have a 10° full-angle of intersection, resulting in a nominal fringe spacing of $2.6\mu m$. The three measurement volumes formed lie along bisectors given as

$$\begin{aligned} \hat{b}_{476.5nm} &= 0.7071\hat{i} + 0.7071\hat{j} \\ \hat{b}_{488nm} &= 0.7071\hat{j} - 0.7071\hat{k} \\ \hat{b}_{514.5nm} &= 0.7071\hat{j} + 0.7071\hat{k} \end{aligned} \tag{6}$$

in tunnel coordinates with x aligned with the freestream velocity, y normal to the floor, and z being the third axis of a right hand system. The velocity and acceleration measurement directions, resulting from the planes of intersection of the laser beams are given also in tunnel coordinates as

$$\begin{aligned} \hat{u}_{476.5nm} &= 0.5\hat{i} - 0.5\hat{j} + 0.7071\hat{k} \\ \hat{u}_{488nm} &= 0.7071\hat{i} - 0.5\hat{j} - 0.5\hat{k} \\ \hat{u}_{514.5nm} &= 0.7071\hat{i} + 0.5\hat{j} - 0.5\hat{k} \end{aligned} \tag{7}$$

A fourth lens, $50.8mm$ in diameter, is used to collect light scattered nominally in the $-y$ direction from the nearly monodisperse $0.6\mu m$ DOP seed particles generated through a vaporization/condensation process. The received light is coupled into a $62.5\mu m$ diameter multimode fiber which is connected to chromatic separation optics that feed the received light to three Hamamatsu model R4124 photomultiplier tubes that convert the three intensity signals to electrical signals. These signals are individually amplified and the signals from the $476.5nm$ and $488nm$ channels are combined into a single signal. The two signals are then simultaneously digitized at 8 bit resolution and $250MS/s$ using a Strategic-Test model UF.258 high speed digitizer board installed in a standard PC. The signals are acquired in bulk, $0.54s$ duration, single-shot records that contain many thousands of bursts. No electronic triggering is used. The data are then permanently stored on swappable IDE hard drives so that signal processing may be done off line.

The signal processor used is software-based and was developed for this project. The processor consists of four important

modules: a burst recognition algorithm, a dual-burst separation algorithm, an FFT-based frequency processor, and an FFT-based chirp processor. The burst recognition algorithm is computationally linear and based upon the time-local root-mean square (RMS) of the signal and the correlation coefficient for a Gaussian fit to the local RMS. This algorithm allows very efficient centering of the signal in the processor window and results in a good estimate of the burst window parameters of the Gaussian model. The dual-burst separation algorithm is similar to the one developed by Nobach (2002), and allows a very high seeding rate to be used since very closely-spaced bursts may be processed. The frequency processor constructs the frequency spectrum for each recognized burst in order to identify the Doppler frequency peak for each channel and interpolate the frequency using a Gaussian fit to three points around the peak. Finally, the chirp processor is the non-parametric technique described by Lehmann et al. (2002) utilizing Gaussian windows and interpolation. Validation for both the frequency and chirp algorithms is done by requiring a normalized signal-to-noise ratio (Shinpaugh et al. 1995),

$$SNR_1 = 10log_{10}\left(N\frac{\sigma^2_{signal}}{\sigma^2_{noise}}\right)dB \tag{8}$$

where σ_i^2 is the variance of i and N is the signal length, be above $20dB$ for all channels simultaneously. Further details of the processor algorithms will also be explained by Lowe (2005).

With conventional LDV techniques, the signal processing step ends when the particle velocity has been estimated by determination of the Doppler frequency. By introducing the additional step to estimate the signal chirp, the technique is extended to allow for Lagrangian particle acceleration estimates. Since the LDV is a zeroth-order instrument a Taylor expansion of the velocity gives:

$$U(t) = f_{Doppler}(t)d = \left(f_0 + \frac{df}{dt}_{t=t_0}(t-t_0) + O[(t-t_0)^2]\right)d \tag{9}$$

where U is the particle velocity measured by the LDV, $f_{Doppler}$ is the Doppler frequency measured, and d is the fringe space which is assumed constant within the measurement volume. Obtaining the chirp, $\frac{df}{dt}_{t=t_0}$, involves higher relative uncertainties than the velocity measurements, so care must be taken to ensure that the LDV system being used will have sufficient dynamic range to distinguish flow accelerations from measurement variance and bias. To do this we desire LDV optics that result in a large number of fringes and a large Rayleigh length for the laser beams resulting in small fringe gradient (Miles 1996). Furthermore, in the current study, near-wall measurements are desired; since the measurement volume diameter must be small to accommodate these measurements, a compromise design must be found. The current LDV achieves this compromise by using relatively large angles for interfering beam pairs, resulting in a small fringe spacing. The nominally spherical $125\mu m$ diameter measurement volume has about 50 fringes for each interference pattern instantaneously, while the gradually focused beams give a Rayleigh length of $95mm$, resulting in negligible fringe gradient bias.

EXPERIMENTAL UNCERTAINTIES

Table 1: Experimental uncertainties.

Term	Uncertainty
U^+	± 0.08
$\overline{u^2}/u_\tau^2$	± 0.11
$\overline{v^2}/u_\tau^2$	± 0.17
$\overline{w^2}/u_\tau^2$	± 0.11
$\overline{uv}/u_\tau^2$	± 0.05
$(\overline{u_i a_j})\nu/u_\tau^4$	± 0.035

Experimental uncertainties have been determined for the statistical quantities reported. These have been estimated by processing two sets of burst data with the same velocity statistics, one set was measured in the flow while the other set was simulated and given the same average burst SNR. The reported uncertainties in table 1 at 20:1 odds are then 1.96 times the RMS variation between the input and output quantities from the simulation.

As with any instrument, knowledge of its limitations is essential. With the present one, the measurement of acceleration must be carefully considered. In the case of those turbulent flows where Taylor's hypothesis is nearly valid, the accelerations become very small and the processor broadening significant. Worse than broadening is the case when the estimation is biased as a function of frequency or chirp rate. Lehmann et al. (2002) show that biases in the acceleration estimation can occur, particularly for small accelerations. This results in a minimum unbiased acceleration measurement for a given flow condition. In particular, dimensional analysis yields the parameter which controls this minimum, given by a ratio, $A(\Delta t)/U$, where A is the true acceleration, Δt is the duration of the burst, and U is average speed of the particle. Thus the minimum acceleration measurable is proportional to the velocity and inversely proportional to the time over which that velocity was observed. With LDV, those two numbers are not completely independent and so a higher average speed results in a shorter observation time. In the case of the turbulent boundary layer, this results in the ability to make low uncertainty measurements near the wall since both the velocity is small there and Taylor's hypothesis is known to fail (Ahn and Simpson 1987). The requirements are further satisfied by complex separating flows where the velocity may be small but large accelerations arise due to the significance of the terms in equation (3).

In order to estimate the uncertainties in the velocity-acceleration correlation, the simulated burst data mentioned above were generated for non-accelerating particles. Therefore, any correlation between the velocities and acceleration measurements represented systematic error in the processor. It was discovered that some scatter in the streamwise velocity-acceleration correlation could be attributed to repeatable, systematic error introduced by the processor. Thus the estimates for the velocity-acceleration correlations were improved by subtracting the zero-acceleration simulation statistics from the flow measurements.

Statistical convergence for each of the quantities reported has been verified and results in deviations much smaller than the uncertainties reported.

Table 2: Flow conditions.

$Re_\theta = 6800$	$U_e = 26.9m/s$
$u_\tau = 1.032m/s$	$\nu/u_\tau = 15\mu m$
$\delta^* = 5.1mm$	$\theta = 3.9mm$
$\delta = 38mm$	$H = delta^*/\theta = 1.30$

RESULTS AND DISCUSSION

Measurements were acquired in a mean 2D constant pressure turbulent boundary layer at $Re_\theta = 6800$. The wind tunnel was adjusted so that the mean core velocity variation was less than $\pm 0.25m/s$ throughout the entire length of the test section. The parameters defining the flow conditions are given in table 2.

All measurements reported were acquired with the advanced LDV system previously described. For each point reported, $8.1s$ of flow data were acquired, though due to data transfer rate limits, each point spans about $2.5min$ of actual time. Each point resulted in $3.8GB$ of raw data which were processed to give time-series for the three components of velocity and acceleration. Statistics were obtained by ensemble-averaging the results with unit weighting. Due to very small correlation coefficients between the velocity and interarrival time, velocity bias was found to be negligible.

Figure 2 is a plot of the mean velocity profiles in wall variables, $U^+ \equiv U/u_\tau$, $y^+ \equiv yu_\tau/\nu$, compared with the data of Ölçmen, Simpson, and Goody (2001) for the same flow at $Re_\theta = 7400$ as well as the DNS of Spalart (1988) at $Re_\theta = 1410$. The wall friction velocity for the present data was determined in two ways, by fitting the log region of the profile to the law-of-the-wall,

$$U^+ = (1/\kappa)ln(y^+) + B \tag{10}$$

where the Coles' constants, $\kappa = 0.41$ and $B = 5.0$, were used, as well as by direct fit to the theoretical viscous sublayer profile for $y^+ < 10$. The values obtained were $1.032m/s$ for the log-layer fit and $0.98m/s$ for the sublayer fit. These values are within the expected uncertainty for wall friction velocity. For the wall-unit normalization, the log-layer fit value was chosen since it resulted in the best collapse with previous results.

The non-zero Reynolds stresses, also in wall coordinates are given in figure 3. These results compare favorably with those of Ölçmen, Simpson, and Goody (2001).

With the considerations from the experimental uncertainties section, the current discussion will be limited to the streamwise velocity-acceleration correlation since the other contributions are much smaller in magnitude in the flat plate boundary layer and on the order of the experimental uncertainties. The measurements for the streamwise velocity-acceleration correlation profile in wall units are given in figure 4. For comparison, the DNS data of Spalart (1988) for the same flow at $Re_\theta = 1410$ and that of Abe et al. (2001) in a turbulent channel at $Re_\tau = 640$ are plotted along with the current data. The measurements show agreement with the low Reynolds number DNS within experimental uncertainties, indicating little Reynolds number effects for this quantity when wall scaling is used. The near wall differences that are seen may be attributed to combinations of uncertainties in the y-distance from the wall, the friction velocity, and the velocity-acceleration correlation.

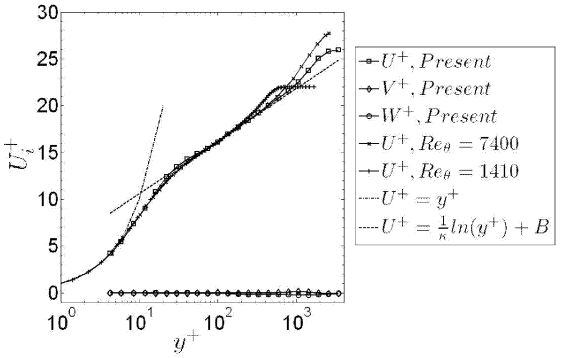

Figure 2: Mean velocity profile in wall units. Data are compared with those of Ölçmen, Simpson, and Goody (2001) for the same flow at $Re_\theta = 7400$ as well as the DNS of Spalart (1988) at $Re_\theta = 1410$.

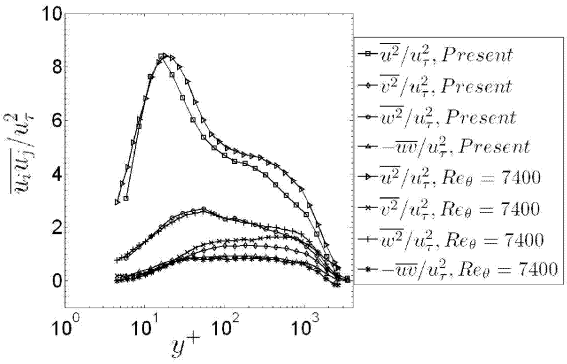

Figure 3: Reynolds stress profiles in wall units. Data are compared with those of Ölçmen, Simpson, and Goody (2001) for the same flow at $Re_\theta = 7400$.

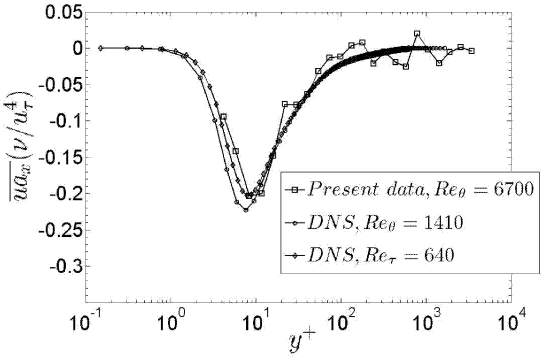

Figure 4: Streamwise velocity-acceleration correlation. Data are compared with DNS of Spalart (1988) and Abe et al. (2001).

The relationship between coherent motions and the velocity-acceleration correlations is considered by decomposing the contributions from the in-plane quadrants. The major contributors to the Reynolds shear stress are the correlated motions known as sweeps which occur for $u > 0, v < 0$ and ejections occurring when $u < 0, v > 0$. It is desired to relate

the sweep and ejection motions in $\overline{uv}$ to the net value of $\overline{ua_x}$. The results from the quadrant analysis are plotted in figure 5. These results indicate that it is the sweep motions that dominate the velocity-acceleration correlation very near wall for $y^+ < 10$. For heights above $y^+ \approx 14$, the contributions switch such that the ejections become dominant in producing the correlation, though the difference is approaching experimental uncertainties. An explanation of the mechanisms for this phenomena is proposed by considering the shape of the probability density functions for the streamwise velocities very near the wall. Figure 6 gives the skewness of the streamwise velocity histograms throughout the profile. It is seen that in the very near wall region the histograms are positively skewed, indicating that the range of positive u' fluctuations is larger than the negative ones. This makes sense intuitively because there is a limit on the lowest velocity since the flow is always downstream, but the greatest possible velocities are related to the higher-momentum large-scale eddies sweeping toward the wall. Note also that the skewness of u' changes sign at the same location that the contributions from sweeps and ejections switch dominance and also where the mean velocity is almost exactly half the freestream value. Heuristically, then, the large difference between the mean velocity very near the wall and the relatively infrequent high-speed sweeps leads to high local viscous shear that acts to limit the convection of momentum that has reached the wall and thus stabilize the mean shear rate in a Lagrangian sense.

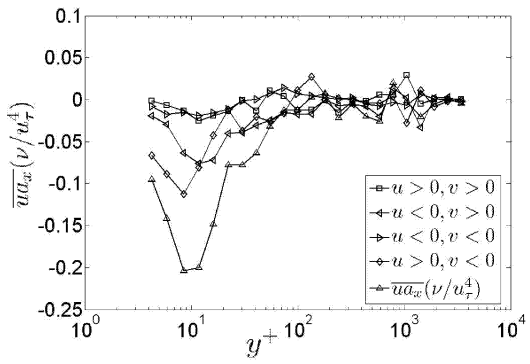

Figure 5: Quadrant analysis of the streamwise velocity-acceleration correlation.

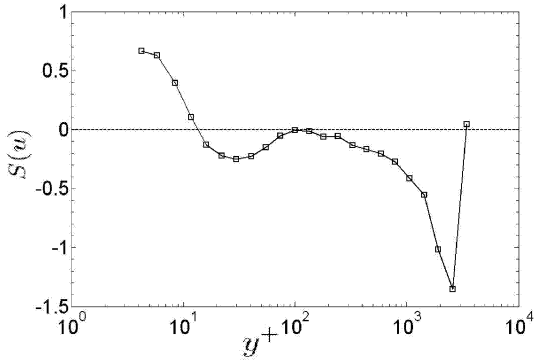

Figure 6: Skewness of the streamwise velocity fluctuation. The dashed line indicates the value for a Gaussian distribution.

An additional feature of the advanced LDV is the ability to measure bursts at very high repetitions. This means that spectra of fluctuating quantities very near the wall may be estimated for a significant range of frequencies. The coherence function between the u and v velocity fluctuations,$\gamma_{uv}^2 = |G_{uv}|^2/(G_{uu}G_{vv})$, as explored by Saddoughi and Veeravalli (1994) for the same flow is plotted in figure 7 with viscous scaling for a range of y^+ values. Since the function is a correlation coefficient in the frequency domain, the range of realizable values is $[0, 1]$. The dominance of $\overline{u^2}$ in the Reynolds stress tensor results in small coherency values near the wall. The coherency continues to increase as the relative value of the shear stress increases, but has begun to decrease before $y^+ = 2566$. It is also seen that there is a common frequency at which the coherency becomes insignificant, about 0.07 in viscous wall units indicating that the frequency of motions which lead to shear stresses in this flow are below this value. In figure 8, the cross-spectra of the u and a_x fluctuations are given for several near-wall points. To our knowledge this is the first report of cross-spectra for the fluctuating velocity and acceleration in a turbulent flow.

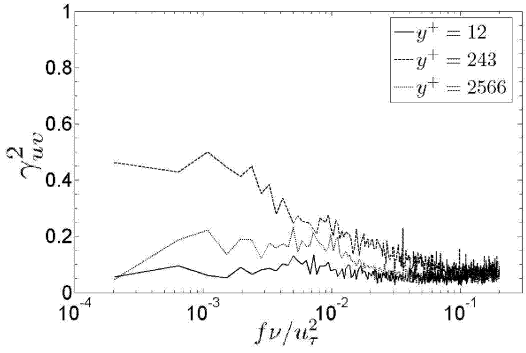

Figure 7: Coherence of the u and v velocity fluctuations in the near wall region.

CONCLUSIONS

An advanced LDV system was developed for measurements of velocity and acceleration statistics in the near wall region of turbulent boundary layers. Using this system measurements have been made in a 2D constant pressure turbulent boundary layer for $Re_\theta = 6800$. The results for mean velocities and Reynolds stresses are consistent with previous data on this flow. The streamwise velocity-acceleration correlation was compared with DNS for this quantity and showed no Reynolds number effects within experimental uncertainties. The relationship between coherent motions and the velocity-acceleration correlation was considered through a quadrant analysis of the quantity. For $y^+ < 14$, the sweep motions result in the greatest contribution to ua_x, which may be attributed to the positively skewed velocity histogram in the very near wall region.

To the authors' knowledge, this study is the first one in which measurements of velocity-acceleration correlations are reported. Therefore, a major goal for the current work was to validate the velocity-acceleration measurements so that the instrument may be applied to more complex 3D flows. The agreement in the near wall region with DNS results for the streamwise correlation give confidence in the application of

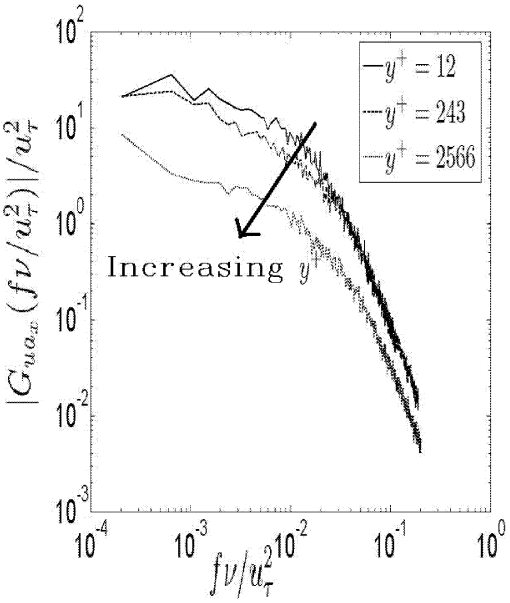

Figure 8: Cross spectra between the u velocity fluctuation and the streamwise acceleration fluctuation, a_x.

technique to other flows. Very importantly, the limitations in the technique have been considered and reveal that reliable measurements will be possible in the near wall region of many complex and separating flows. In current work, improvements are being made to the probe that will result in measurements of lower-magnitude accelerations as well as direct measurement of the velocity gradient tensor. Using the state-of-the-art hardware, future studies will reveal the structure of dissipation and velocity pressure-gradient correlations in many complex flows which have never been examined to that extent.

ACKNOWLEDGMENTS

The authors gratefully acknowledge the support provided for this work by AFOSR grant F49620-03-1-0057 under program manager, Dr. T. Beutner.

REFERENCES

Ahn, S. and Simpson, R.L. 1987, "Convective wave speed and spectral features of turbulent boundary layers" *AIAA* 25^{th} *Aerospace Sciences Meeting*, Paper AIAA-87-0198, Jan. 12-15, Reno, NV.

Abe, H., Kawamura, H., and Matsuo, Y. 2001, "Direct numerical simulation of a fully developed turbulent channel flow with respect to the Reynolds number dependence," *J. Fluids Engr.*, Vol. 123, pp. 382-393

Bennington, J. L, 2004, "Effects of various shaped roughness elements in two-dimensional high Reynolds number turbulent boundary layers." M.S. Thesis, Virginia Tech, Blacksburg, VA.

Christensen, K.T. and Adrian, R.J. 2002 "The velocity and acceleration signatures of small-scale vortices in turbulent channel flow." *J. Turb.* Vol. 3, paper 023.

Coleman, G. N., Kim, J, and Spalart, P.R., 2000 "A numerical study of strained three-dimensional wall-bounded turbulence" *J. Fluid Mech.*, Vol. 416, pp. 75-116.

DeGraaff, D.B. and J.K. Eaton, 2000, "Reynolds Number Scaling of the Flat-Plate Turbulent Boundary Layer," *J. Fluid Mechanics*, Vol. 422, 319-346.

Hill, R.J. and Thoroddsen, S.T. 1997 "Experimental evaluation of acceleration correlation for locally isotropic turbulence." *Physical Rev. E* Vol. 55, No. 2, pp. 1600-1606.

LaPorta, A, Voth, G.A., Crawford, A.M., Alexander, J. and Bodenschatz, E. 2001 "Fluid particle accelerations in fully developed turbulence." *Nature* Vol. 409, pp. 1017-1019.

Lehmann, B., Nobach, H., and Tropea, C. 2002, "Measurement of acceleration using the laser Doppler technique." *Meas. Sci. Technol.* 13, 1367-1381.

Lowe, K.T. 2005 "Design and application of an advanced Laser Doppler Velocimeter for high-order measurements in turbulent boundary layers," Ph.D. dissertation, Virginia Tech, Blacksburg, VA.

Miles, P.C., 1996, "Geometry of the fringe field formed in the intersection of two Gaussian beams." *Appl. Optics*, Vol. 35, No. 30, pp. 5887-5895.

Nobach, H. 2002 "Analysis of dual-burst laser Doppler signals", *Meas. Sci. Technol. 13*, 33-44.

Ölçmen, S., Simpson, R., Goody, M. 2001 "An experimental investigation of two-point correlations in two- and three-dimensional turbulent boundary layers" *Flow, Turb. and Combustion 66*, pp. 85-112.

Pope, S. 2000 *Turbulent Flows*, Cambridge University Press.

Saddoughi, S. and Veeravalli, S., 1994 "Local isotropy in turbulent boundary layers at high Reynolds number" *J. Fluid Mech.*, Vol. 268, pp. 333-372.

Shinpaugh, K.A., Simpson, R.L., Wicks, A.L., Ha, S.M., and Fleming, J.L. 1992, "Signal-processing techniques for low signal-to-noise ratio laser Doppler velocimetry signals," *Experiments in Fluids*, Vol. 12, pp 319-328.

Spalart, P. 1988, "Direct simulation of a turbulent boundary layer up to $Re_\theta = 1410$," J. Fluid Mech., Vol. 187, pp. 61-98.

Vedula, P. and Yeung, P.K. 1999 "Similarity scaling of acceleration and pressure statistics in numerical simulations of isotropic turbulence." *Phys. Fluids* Vol. 11, pp. 1208-1220.

Virant, M and Dracos, T. 1997 "3D PTV and its application on Lagrangian motion." *Meas. Sci. Technol.* Vol. 8, pp. 1539-1552.

Voth, G.A. Satyanarayan, K., and Bodenschatz, E. 1998 "Lagrangian acceleration measurements at large Reynolds numbers." *Phys. Fluids* Vol. 10, pp. 2268-2280.

Voth, G.A., LaPorta, A., Crawford, A.M., Alexander. J. and Bodenschatz, E. 2002 "Measurement of particle accelerations in fully developed turbulence." *J. Fluid Mech.* Vol. 469, pp. 121-160.